



# Parametric study and techno-economic analysis of a novel integration between thermoelectric generator and organic Rankine cycle onboard passenger ship

Ahmed G. Elkafas<sup>1,2</sup>

Received: 3 December 2023 / Accepted: 4 April 2024 / Published online: 17 June 2024  
© Akadémiai Kiadó, Budapest, Hungary 2024

## Abstract

The International Maritime Organization has set targets for reducing greenhouse gas emissions from ships. Thus, it is imperative to investigate novel technologies that have the potential to achieve these targets and reduce emissions in the short and long term. Waste heat recovery (WHR) technology, which generates electricity from engine waste energy, is a promising solution. This research examines the integration of a thermoelectric generator and organic Rankine cycle as a combined WHR system onboard a passenger ship. The purpose of the paper is to analyze the TEG–ORC system parametrically and from a techno-economic perspective. The results showed that the optimum design scenario is achieved by integrating the recuperative ORC system (rcORC) with the TEG system, this integration produces 1569 kW as net output power (19% more than the original TEG–ORC system) at an evaporation pressure of 55 bar. The exergy efficiency of the system is enhanced from 43.2 to 48.6% by the addition of the recuperator. Also, the efficiency of the power system (engine + TEG–rcORC system) is 53.2% (+6.1% over the efficiency of the standalone engine). The integration of the TEG–rcORC system with the main engine provides the ship with an energy efficiency existing index (EEXI) of 22.47 g-CO<sub>2</sub> ton<sup>-1</sup> nm<sup>-1</sup>, this value is lower than the required EEXI by 11%. From an economical point of view, the levelized power cost of the TEG–rcORC system is 280.2 € kW<sup>-1</sup>, and the annual saving in expenses is 1.05 M€ with a discounted payback time of 3.9 years.

**Keywords** Waste heat recovery · Ship energy efficiency · Fuel saving · Thermoelectric generator · Organic Rankine cycle · Passenger ship

## Introduction

The maritime transportation sector encouraged the enhancement of energy efficiency and greenhouse gas (GHG) emission reduction by promoting the adoption of several energy efficiency measures. These measure adoption was stimulated by recent statistics on the emission levels from ships. Based on the fourth IMO GHG study in 2020 [1], the GHG emissions (carbon dioxide (CO<sub>2</sub>), methane, and nitrous oxide) from the global fleet of ships (including domestic vessels

and international shipping) have increased to 1,076 Mt of CO<sub>2</sub>e in the fiscal year of 2018. For the CO<sub>2</sub> emissions after 2018, the data collected by the Data Collection System of IMO showed that the CO<sub>2</sub> emissions from ships of or greater than 5000 gross tonnage (GT) was 662 Mt CO<sub>2</sub> in 2019 based on consumption of 213 Mt of fuel from 27,221 ships and 660 Mt CO<sub>2</sub> in 2021 based on consumption of 212 Mt of fuel from 28,171 ships [2]. Therefore, IMO has released several regulations and rules to control ship emissions, firstly by placing a target in 2018 for reducing GHG emissions by 50% in 2050 compared to 2008 levels [3], then this target has been enhanced in their recent strategy in 2023 [4] to achieve carbon neutrality (zero emissions) in 2050 with reducing these emissions by 30% in 2030 and 80% in 2040.

At the European Union (EU) level, ships emit about 3–4% of the total CO<sub>2</sub> emissions emitted inside the EU, the contribution of maritime transportation was around 124 Mt in 2021 [5]. To prevent these emissions from growing in the future, the European Commission agreed to extend the

✉ Ahmed G. Elkafas  
ahmed.elkafas@edu.unige.it

<sup>1</sup> Thermochemical Power Group (TPG), DIME, University of Genoa, 16145 Genoa, Italy

<sup>2</sup> Department of Naval Architecture and Marine Engineering, Faculty of Engineering, Alexandria University, Alexandria 21544, Egypt

EU-Emission trading system (ETS) to cover the CO<sub>2</sub> emissions emitted from maritime transportation (ships with 5000 GT or above) to help in achieving a carbon neutrality target in 2050. This extension started in January 2024 to cover 100% of emissions from ships that have trips between two European ports and 50% of emissions from ships sailing between a European port and another port outside the EU [6].

To reach the decarbonization targets of IMO and EU, various approaches could be implemented including technical and operational measures [7–9]. These approaches could be divided into improving the engine design and efficiency management (such as hybrid diesel-electric; enhanced fuel injection system; and waste heat recovery (WHR) systems, CO<sub>2</sub> emission reductions of 3–8%), utilization of alternative propulsion technologies (such as pre-swirl; contra-rotating propellers; etc., 0.5–15% reduction of CO<sub>2</sub>), developing innovative assistance propulsion systems onboard ships (flattener rotors; solar panels; etc., 0.5%–50% reduction of CO<sub>2</sub> emissions), voyage optimization (such as speed reduction; hull cleaning; weather routing; etc., 0–38% reduction of CO<sub>2</sub> emissions), and utilization of alternative clean fuels (for example, hydrogen; natural gas; methanol; and ammonia; up to 100% reduction of CO<sub>2</sub> emissions) [7–9].

Conventional internal combustion engines (ICEs) powered by fossil fuels (heavy fuel oil (HFO) or marine diesel oil (MDO)) are considered the main power plant used onboard ships [10]; however, over 50% of the fuel energy combusted in these engines lost in exhaust gases, lubricating oils, scavenging air, and cooling water [11, 12]. Therefore, implementing WHR technologies to capture the wasted energy from ICEs is considered an effective approach to increase energy efficiency and reduce fuel consumption which results in the reduction of CO<sub>2</sub> emissions. In addition, the installation of WHR technologies onboard ships could be done without major modifications to the existing engine rooms onboard and is easier than the installation of innovative energy systems or utilization of dual fuel engines in terms of capital expenses [13].

In the literature, there are several researchers reviewed the WHR technologies for maritime applications like shu et al. [14] and singh and Pedersen [12] who classify the different WHR technologies including turbocompound systems, absorption refrigeration systems, steam Rankine cycles (SRC), organic Rankine cycles (ORC), thermoelectric generators (TEG), and Kalina cycles (KC). Moreover, Palomba et al. [15] assessed whether it would be feasible to use WHR to power cooling and refrigeration equipment on fishing boats, as well as offering recommendations for system layouts and convergence. In contrast, Xu et al. [16] examined all the options available for onboard cold storage, mainly focusing on elements and generally classifying them as absorption, adsorption, and hybrid refrigeration systems.

Regarding the application of ORC in the maritime sector, Song et al. [17] have studied the utilization of the jacket cooling water and exhaust gases for preheating and vaporization of the operational fluid of ORC. Baldi [18] has examined the installation of an ORC onboard chemical tanker and found that its application can reduce fuel consumption by 11.4%. Mondejar et al. [19] found that the best heat sources from ICE to be used for ORC are flue gases and jacket cooling water. Lion et al. [20] examined the ORC implication onboard ships by using heat energy available in the exhaust gases and scavenging air. Moreover, the high-temperature cooling water has been used to preheat the working fluid in three different ORC designs by Casisi et al. [21]. Additionally, a study by [22] proposed the utilization of a WHR system based on ORC on board an oil tanker ship combined with main engines and auxiliary engines powered by methanol, and LNG, respectively. It finds that the attained energy efficiency existing ship index (EEXI) and carbon intensity indicator (CII) have been reduced to fulfill the current requirements and maintain the oil tanker's CII rating at levels B–C.

Furthermore, TEG systems have been applied in aviation, automobile, and marine fields [23–26] thanks to their durability, low maintenance needs, ecologically consciousness, and compatibility integrated with other WHR technologies such as ORC. Using a set of experimental records, Kristiansen et al. [27] looked at the installation of TEGs inside a bulk carrier. Their findings showed that 133 kW could be restored from several waste heat supplies with various qualities. Moreover, Georgopoulou et al. [28] found that up to 26 kW can be recovered by using TEG which absorbs the waste heat available at the scavenging air and exhaust gases from the main and auxiliary engines, respectively.

To obtain an improved performance and output power from the waste heat sources available onboard ships, it is recommended to integrate WHR systems to achieve energy and cost-efficient zero waste heat. There are some efforts in the integration of the ORC and KC as presented in [29] where the authors propose their integration in a combined WHR system to recover waste energy available in the exhaust gas and jacket water waste heat from a combined heat and power engine. The study examined the optimal values of different parameters to be used for KC. Moreover, the study's results concluded that the net power output from the combined WHR system was equal to 211 kW (divided into 168.69 kW for KC and 42.34 kW for ORC) with thermal efficiency equal to 26.5% and the payback period is 4.2 years.

Moreover, there is another contribution by He et al. [30], they conducted an experimental campaign to study the integration between ORC and KC in a combined WHR system from an ICE and examine this integration from energy balance and exergy analysis perspectives. Furthermore, the

ORC has been integrated with SRC and power turbine to generate more power by using the waste heat available in marine low-speed diesel engines as shown in [31]. The study proposed the utilization of exhaust gas from diesel engines as a high-temperature heat source to power the power turbine and the installed turbocharger in the diesel engine.

Based on the findings from this literature survey, it is found that a single WHR system has limits in generating power from various waste heat sources from ICEs. One of the difficulties of recovering waste heat like exhaust gases onboard ships by using ORC is exhaust gases' temperature, which is considered a high one and results in a huge temperature gradient between it and the working fluids. Moreover, the decomposition temperature of most of the working fluids that can be used in ORC gives the limitation to benefit the full of the exhaust gases onboard ships because the working fluid can be resolved at a temperature higher than that one.

In order to avoid these limitations in recovering the waste heat sources from marine ICEs, the paper integrates TEG and ORC in a combined WHR system onboard a passenger ship. The combined WHR system will be investigated by conducting parametric analysis and techno-economic approaches and employing energy efficiency, exergy efficiency, levelized power cost, discounted payback time, and EEXI as key performance indicators. The parametric analysis is conducted via MATLAB by investigating the effect of various parameters including working fluid specifications, TEG scale, evaporation pressure, and temperature on the system performance.

## Description of case study and WHR system

### Case study description

The case study is selected to be a Ro-Ro Passenger ship that is called "Europa Palace" [32, 33]. The ship is operated in the western Mediterranean Sea in Europe between Greece and Italy ports. The passenger capacity is 1800 distributed into 242 cabins, 8 superior cabins, and 48 armchairs. Moreover, the garage capacity onboard the ship is 2200 l m<sup>-1</sup> which can carry up to 870 vehicles. The summer deadweight and gross tonnage equal 6515 tons and 32,728 tons, respectively. The ship's length and breadth are 204 m and 25 m, respectively. The ship speed service is 29 knots.

The ship is propelled by using four marine diesel engines from Wartsilla, and there are another three diesel generators. Because the proposed waste heat recovery system will be installed to convert the wasted heat from the main engines onboard the ship into electrical power, the main parameters of the main engine are shown in Table 1 [34].

Based on the datasheet of Wartsila 12V46F [34], the waste heat of the engine is divided into five streams including exhaust gases, lubrication oil, jacket water cooling,

**Table 1** The main parameters of the installed engine onboard the ship

Parameter	Value
Main engine type	Wartsila 12V46F
Rated output power at 85% load/kW	12,240
Number of cylinders	12
Engine speed/rpm	600
Combustion air mass flow rate/kg s <sup>-1</sup>	25.1
Specific fuel consumption/g kWh <sup>-1</sup>	175
Exhaust gas mass flow rate/kg s <sup>-1</sup>	22.2
Exhaust gas temperature/K	609
Jacket cooling water heat/kW	1530
Jacket water temperature/K	353

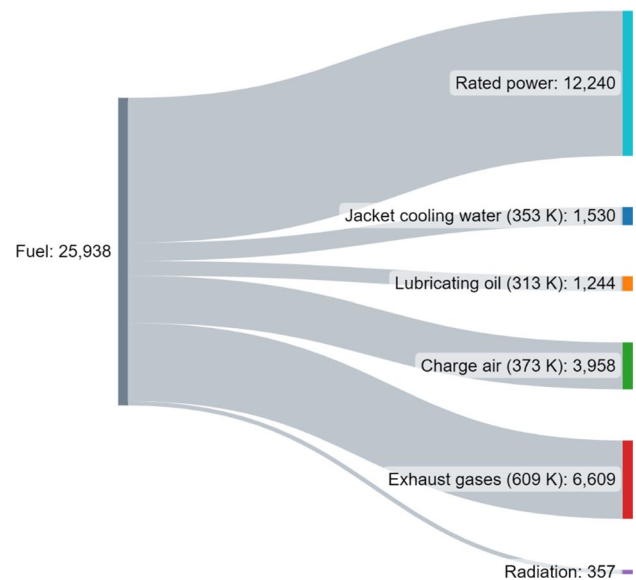


**Fig. 1** Sankey diagram of the engine (Wartsila 12V46F) at 85% load, the values of heat and power are expressed in kW

charge air, and radiation. Figure 1 shows the Sankey diagram of the engine at 85% load as it describes the distribution of heat flows and power while mentioning their temperatures. It is noted that the lubricating oil temperature is 313 K which can be neglected to be used as a waste heat source to be recovered through the proposed WHR system. The exhaust gases contribute about 25.5% of fuel energy, while jacket cooling water and scavenge air contribute about 5.9% and 15.3%. Moreover, the generated power from the engine at 85% load is 12,240 kW and by evaluating the efficiency is found to be equal to 47.2%.

In the paper, it is proposed to install the combined TEG–ORC system to absorb the wasted energy in the exhaust gas and jacket water heat from one main engine. The analysis aims to investigate the effect of changing different working parameters on the performance of the combined

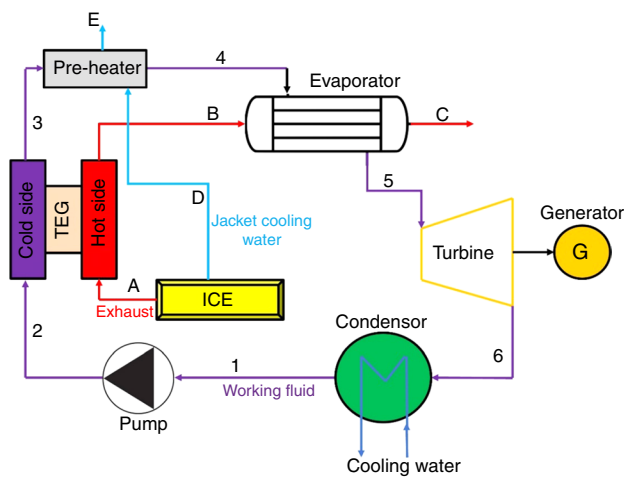


Fig. 2 Diagram of TEG–ORC system installed with ICE

TEG–ORC system; therefore, the engine is assumed to be operated under rated conditions as shown in Table 1.

### Description of TEG–ORC combined system

In this paper, the waste heat from ICE is proposed to be recovered by using an integration between TEG and ORC as expressed in Fig. 2. The WHR system has the following components: evaporator, turbine, condenser, pump, TEG, and preheater. The working fluid is condensed in the condenser to be pumped by using a pump that increases the pressure of the working fluid to the evaporator pressure. Then the high-pressure fluid is preheated in the cold side of TEG by absorbing the heat supplied in the TEG’s hot side from high-temperature exhaust gases. The working fluid’s temperature increases by entering a preheater located between TEG and the evaporator which uses the main engine’s jacket cooling water as a heat source. After that, the organic fluid enters the evaporator in which the organic fluid is converted to be in the gas phase by using the exhaust gases as a heat source at constant temperature. Then, the superheated vapor enters the turbine in which the kinetic energy of high-pressure vapor is converted to mechanical energy, then converted to electrical power by using a generator. The low-pressure vapor enters the condenser to be liquified again to complete the cycle.

In the current study, there is another configuration for the combined cycle by integrating TEG with recuperative ORC (rcORC), this configuration will be called TEG–rcORC. The recuperator is proposed to be added after the stream coming from the ORC turbine and before the TEG as shown in Fig. 3. The hot side of the recuperator will be fed by the exhaust vapor extracted from the ORC turbine while the cold side will be fed by the cold working fluid coming out from the pump. The cold working fluid from the pump is

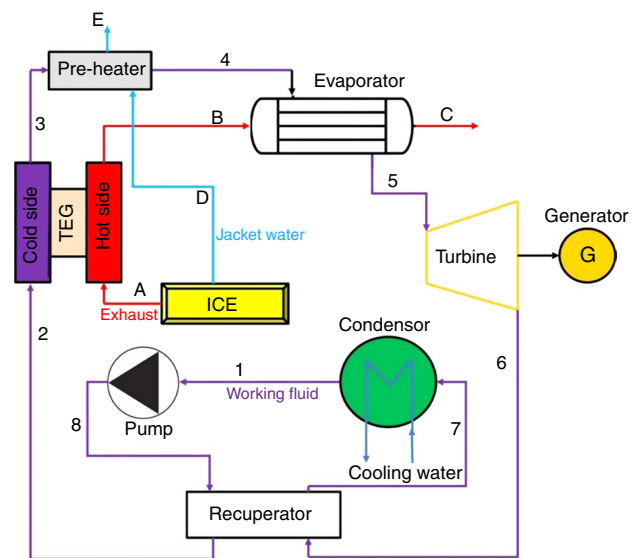


Fig. 3 Diagram of TEG–rcORC system installed with ICE

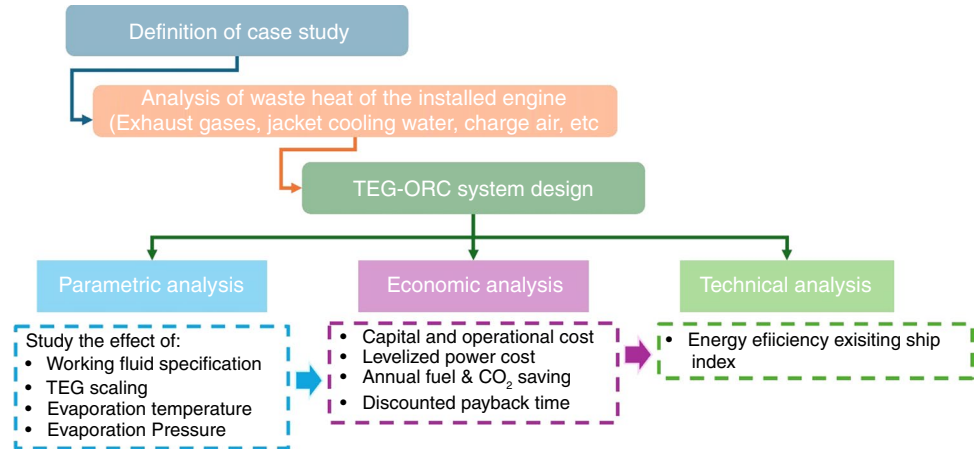
considered a high-pressure fluid, therefore, it can exchange heat with the high-temperature vapor that comes out from the turbine.

### Methodology

The current paper assesses the performance of the TEG–ORC system by using parametric and techno-economic approaches via a methodology consisting of different phases as shown in Fig. 4. These phases have been modeled and simulated in MATLAB software.

The first phase is to identify the case study (ship) by reporting its main specifications and the installed ICE onboard. Then, the second phase is to analyze the waste heat that exists from the engine by describing its Sankey diagram and reporting the temperature and quantities of waste heat at the design point. After that, the description of the TEG–ORC system configuration considers the available waste heat flows to be captured from the engine. Then, the parametric analysis is conducted through thermal modeling of the combined system and studying the effect of different parameters on the system performance, these parameters include the working fluid specifications, TEG scaling, evaporation pressure, and temperature. Also, the effect of these parameters will be studied from an economic point of view by evaluating the capital expenses of the system in different cases. Then, the economic assessment will be done through the evaluation of levelized power cost, annual fuel or CO<sub>2</sub> savings, and discounted payback time. Finally, the technical analysis will be conducted by studying the effect of the TEG–ORC system installation on the EEXI of the ship.

**Fig. 4** The methodological approach for the assessment of the TEG–ORC system



**Thermal modeling of the combined system**

A few presumptions underpin the thermodynamic study, including the disregard for heat leakage in the condenser and heat exchanger, the constant pressure during evaporation and condensation, and the disregard for the preheater’s internal resistance. Every system component is viewed as a control volume for energy modeling, and the laws of thermodynamics are applied accordingly. The energy balance equation can be applied to each part of the suggested system as indicated by Eq. (1) [35].

$$\dot{Q}_{C.V} - \dot{W}_{C.V} = \sum \dot{m}_{out} * h_{out} - \sum \dot{m}_{in} * h_{in} \quad (1)$$

where  $\dot{Q}_{C.V}$  and  $\dot{W}_{C.V}$  represent the power work and heat rate that exist in the control volume. While  $\dot{m}$  and  $h$  are the mass flow rate and the enthalpy of the working medium, respectively at the inlet (in) and outlet (out) of the control volume. There are several components in the proposed system, therefore, the thermodynamic formula of each one is shown in Table 2. Where the subscripts p, wf, ex, hs, pre, ev, T, cond, and rec refer to the pump, working fluid, exhaust gas, the hot

side of TEG, preheater, evaporator, turbine, condenser, and recuperator, respectively.

Based on the Seebeck effect, the thermodynamic modeling of TEG can be established by defining the cold side that releases heat from its interaction with the ORC working medium and the hot side that absorbs the heat from the exhaust gases. The energy balance formulas that are used to calculate the rate of heat released ( $\dot{Q}_C$ ), and the hot absorption ( $\dot{Q}_H$ ) inside the TEG are presented in Eq. (12–13) [39].

$$\dot{Q}_C = n \left[ \alpha_{NP} * T_c * I_o + K_o (T_h - T_c) + \frac{I_o^2 * R_o}{2} \right] = n * \frac{T_c - T_{ORC}}{r_c} \quad (12)$$

$$\dot{Q}_H = n \left[ \alpha_{NP} * T_h * I_o + K_o (T_h - T_c) + \frac{I_o^2 * R_o}{2} \right] = n * \frac{T_A - T_h}{r_h} \quad (13)$$

In Eqs. (12–13), there are some coefficients such as the Seebeck coefficient ( $\alpha_{NP}$ ) and the thermal conduction coefficient ( $K_o$ ), while there are some parameters for the thermoelectric couple such as the thermal resistance ( $r_h$ ), the current flow ( $I_o$ ), and the electrical resistance ( $R_o$ ). The heat

**Table 2** Thermodynamic balance equations for different components [36–38]

Component	Formula	Equation no
Pump	$\dot{W}_p = \dot{m}_{wf} \times (h_2 - h_1), \eta_{pump} = \frac{v_1 * (P_2 - P_1)}{h_2 - h_1}$	(2)
The hot side of TEG	$\dot{Q}_{hs,TEG} = \dot{m}_{ex} \times (h_A - h_B)$	(3)
Preheater	$\dot{Q}_{pre} = \dot{m}_{wf} \times (h_4 - h_3) = \dot{m}_{jw} \times (h_D - h_E)$	(4)
Evaporator	$\dot{Q}_{ev} = \dot{m}_{wf} \times (h_5 - h_4) = \dot{m}_{ex} \times (h_B - h_C)$	(5)
Turbine	$\dot{W}_T = \dot{m}_{wf} \times (h_5 - h_6)$	(6)
Condenser	$\dot{Q}_{cond} = \dot{m}_{wf} \times (h_1 - h_6)$	(7)
Recuperator	$\dot{Q}_{rec} = \dot{m}_{wf} \times (h_6 - h_7) = \dot{m}_{wf} \times (h_8 - h_2)$	(8)
ORC	$\dot{W}_{ORC} = \dot{W}_T - \dot{W}_p$	(9)
ORC efficiency	$\eta_{ORC} = \frac{\dot{W}_{ORC}}{\dot{Q}_{ev} + \dot{Q}_{pre}}$	(10)
TEG–ORC efficiency	$\eta_{TEG-ORC} = \frac{\dot{W}_{TEG} + \dot{W}_{ORC}}{\dot{Q}_{ev} + \dot{Q}_{pre} + \dot{Q}_{hs,TEG}}$	(11)

loss is neglected as assumed in the proposed configuration so that the conversion efficiency of TEG can be estimated based on  $\dot{Q}_C$  and  $\dot{Q}_H$ .

Based on the theory of efficient liquid-based electricity generation apparatus inside thermoelectric, the efficiency of TEG can be evaluated as shown in Eq. (14) [40].

$$\eta_{\text{TEG}} = \left(1 - \frac{T_L}{T_H}\right) * \frac{\sqrt{1 + ZT_M} - 1}{\sqrt{1 + ZT_M} + \frac{T_L}{T_H}} \quad (14)$$

where  $ZT_M$  is a variable governs the internal conversion efficiency of TEG, while  $T_L$  and  $T_H$  are the mean temperature across the cold side and hot side of TEG, respectively.

The second law of thermodynamics is given more consideration when assessing the system performances since it offers more insightful analysis. The total exergy of a fluid stream may be expressed as shown in Eq. (15) by ignoring the chemical, kinetic, and potential exergies while considering the physical exergy only [35].

$$\dot{E}_j = \dot{E}_{j,\text{ph}} = \dot{m}_j * [(h_j - h_0) - T_0(s_j - s_0)] \quad (15)$$

where ( $\dot{E}_j$ ) is the exergy rate measured in kW, ( $T_0$ ) is the temperature, and ( $s$ ) is the entropy. The subscript ( $j$ ) can be replaced by the different state points. The exergy efficiency ( $\eta_{\text{exergy}}$ ) of the proposed system can be evaluated as shown in Eq. (16) by considering the waste heat from exhaust gases and jacket cooling water as the exergy input to the system [41, 42].

$$\eta_{\text{exergy}} = \frac{\dot{W}_{\text{TEG}} + \dot{W}_{\text{ORC}}}{\dot{E}_{\text{in}}} = \frac{\dot{W}_{\text{TEG}} + \dot{W}_{\text{ORC}}}{\dot{m}_{\text{ex}} * (h_A - h_C) + \dot{m}_{\text{jw}} * (h_D - h_E)} \quad (16)$$

For each component in the system, the exergy loss rate can be evaluated by applying the exergy balance equation as shown in Eq. (17) [43].

$$\dot{E}_{\text{loss},i} = \sum \dot{E}_{\text{in},i} - \sum \dot{E}_{\text{out},i} \quad (17)$$

where  $\dot{E}_{\text{loss},i}$  is the rate of exergy loss in kW for component ( $i$ ). The overall exergy loss from the proposed system can be evaluated by summing the exergy losses from all components.

### Economic modeling of the combined system

The economic assessment modeling relates the system cost to the system ineffectiveness and the working environment properties. In this paper, the production cost of electricity is divided into two sources (ORC and TEG). For each component, there are two cost categories that will be considered, the capital expenses (CapEx) and operation/maintenance expenses (OpEx). Moreover, the economic

modeling will depend on some operational factors such as the operation time ( $T_o$ ), number of years ( $N$ ), and the interest rate ( $i$ ).

The economic assessment is achieved in the current study by evaluating the levelized power cost (LPC) that is calculated by dividing the total expenses including CapEx and OpEx by the generated power. Because the investigated combined WHR system includes two different systems (ORC and TEG), the LPC will be studied twice. Firstly, the levelized power cost of ORC may be evaluated by using Eq. (18) [44].

$$\text{LPC}_{\text{ORC}} = \frac{\text{CapEx}_{\text{ORC}} * (i * (1 + i)^N / (1 + i)^N - 1) + \text{OpEx}_{\text{ORC}}}{\dot{W}_{\text{ORC}} * T_o} \quad (18)$$

where  $\text{LPC}_{\text{ORC}}$  is the levelized power cost of ORC ( $\text{\$/kWh}^{-1}$ ),  $\text{CapEx}_{\text{ORC}}$  is the capital expenses of ORC system, and  $\text{OpEx}_{\text{ORC}}$  is the operational expenses including the maintenance cost of ORC system. Although there is no direct formula to calculate the capital cost of ORC, it can be evaluated by calculating the base cost of its components such as condenser, evaporator, turbine, preheater, and pump. The capital cost of these components ( $CA_{i,\text{base}}$ ) can be evaluated as shown in Table 3 [45, 46], in which ( $A$ ) represents the surface area measured in  $\text{m}^2$ .

The area ( $A$ ) of different components like evaporator, condenser, and preheater can be calculated by using Eq. (19) [49].

$$A_i = \frac{Q_i}{\text{LMTD}_i * U_i} \quad (19)$$

where  $\text{LMTD}_i$  is the logarithmic mean temperature difference of the heat exchanger ( $i$ ), while  $U_i$  is the overall heat transfer coefficient for evaporator, condenser, and preheater that assumed to be 99, 764, and  $524 \text{ W m}^{-2} \text{ K}^{-1}$ , respectively [50].

The capital cost of each component defined in Table 3 should be calculated at the present year, this can be done by converting the capital cost from the base year to the present year by using the Chemical Engineering Plant Cost Index (CEPCI) as shown in Eq. (20) [51].

**Table 3** The capital cost of different components [45, 47, 48]

Component	Capital cost/ $CA_{i,\text{base}}$
Evaporator	$CA_{\text{ev}} = 309.14 \times A_{\text{ev}}^{0.85}$
Condenser	$CA_{\text{cond}} = 516.62 \times A_{\text{cond}}^{0.6}$
Pump	$CA_{\text{p}} = 3540 \times \dot{W}_{\text{p}}^{0.71}$
Preheater	$CA_{\text{ph}} = 10,000 + 324 \times A_{\text{ph}}^{0.91}$
Turbine	$CA_{\text{T}} = 4750 \times \dot{W}_{\text{T}}^{0.75}$
Thermoelectric generator	$CA_{\text{TEG}} = 1000 \times \dot{W}_{\text{TEG}}$

$$CA_{i,present} = CA_{i,base} \times \frac{CEPCI_{present}}{CEPCI_{base}} \tag{20}$$

where  $CEPCI_{present}$  is the Chemical Engineering Plant Cost Index for the present year (2023) that is considered to be about 800 [52], while  $CEPCI_{base}$  is the Chemical Engineering Plant Cost Index for the present year (2010) that is considered to be about 522 for all components instead of evaporator that is assumed to be 390 [47]. Furthermore, the levelized power cost of TEG system may be evaluated as shown in Eq. (21).

$$LPC_{TEG} = \frac{(CapEx_{TEG} + CA_{pipe}) * ((i * (1 + i)^N / (1 + i)^N - 1)) + OpEx_{TEG}}{\dot{W}_{TEG} * T_o} \tag{21}$$

where the capital cost of TEG is calculated as shown in Table 3, while the capital cost of the exhaust pipeline ( $CA_{pipe}$ ) can be evaluated based on the equation of preheater as described in Table 3.

For maritime applications, the implementation of this kind of WHR system onboard ships leads to economic benefits in terms of reduction in operational expenses including the reduction in fuel expenses resulting from the generated power from the wasted energy of engines. Moreover, this reduction in fuel consumption resulted in a reduction of CO<sub>2</sub> emissions which leads to a reduction in CO<sub>2</sub> taxes following EU-ETS in Europe. These benefits are combined in one formula as shown in Eq. (22) in which ( $AS_{fuel-CO_2}$ ) is the annual savings in fuel expenses and CO<sub>2</sub> taxes.

$$AS_{fuel-CO_2} = \sum_{trips} W_{TEG-ORC} * T_o * SFC_{DG} * (CA_{fuel} + CF_f * CT_{CO_2}) * 10^{-3} \tag{22}$$

where  $W_{TEG-ORC}$  is the net electric power produced from the TEG–ORC system in kW,  $T_o$  is the planned sailing time of trip in hours,  $SFC_{DG}$  is the specific fuel consumption for the installed diesel generator onboard ship (kg kWh<sup>-1</sup>),  $CA_{fuel}$  is the diesel fuel cost (€ ton<sup>-1</sup>),  $CF_f$  is the conversion factor between diesel fuel and CO<sub>2</sub>, and  $CT_{CO_2}$  is the cost of 1 ton of CO<sub>2</sub> emitted (€ ton<sup>-1</sup>) based on EU-ETS requirements [6].

Moreover, one of the crucial economic indicators for the installation of the proposed WHR system is the discounted payback time (DPT). It can be calculated based on the annual saving of the operational expenses resulting from the operation of the TEG–ORC system. The DPT in the present study can be evaluated as shown in Eq. (23) [50].

$$DPT_{TEG-ORC} = - \frac{\ln \left[ 1 - \frac{CapEx_{TEG-ORC}}{AS_{fuel-CO_2}} * (e^i - 1) \right]}{i} \tag{23}$$

where  $CapEx_{TEG-ORC}$  is the total capital expenses of the combined system after applying the inflation effect by using the

same formula in Eq. (20), and (i) is the interest rate that assumed to be 4%.

### Technical analysis approach

The technical analysis of the TEG–ORC system can be accomplished by investigating the effect of the addition of this kind of WHR system on energy efficiency by using technical regulatory indicators as recommended by IMO. EEXI is the regulatory indicator for the in-service fleet like the investigated case study. The attained EEXI is an indicator to assess the ship performance in terms of energy efficiency (g-CO<sub>2</sub> ton<sup>-1</sup> nm<sup>-1</sup>) and its value must be equal to or less than the calculated required EEXI to comply with the IMO rules and regulations. The required EEXI can be calculated as shown in Eq. (24) [53].

$$EEXI_{req} = a * DWT_{ship}^{-c} * (1 - \frac{X}{100}) \tag{24}$$

where DWT is the deadweight of ship in tons, and (a and c) are constant factors that vary with the type of ship to calculate the reference line of EEXI (for RO-RO passenger ship, they are equal to 752.16 and 0.381, respectively). While X is a reduction factor, its value is based on the ship type and its capacity (for the investigated case study, its value is 5%) [54].

While the attained EEXI that must be lower than the required EEDI can be estimated as shown in Eq. (25) [55], this equation has been simplified in comparison to the original one.

$$EEXI_{att} = \frac{f_j * P_{ME} * CF_{ME} * SFC_{ME} + (P_{AE} - \sum_{i=1}^{n_{eff}} f_{eff,i} * P_{AE,eff,i}) * CF_{AE} * SFC_{AE}}{f_c * DWT_{ship} * V_R} \tag{25}$$

where  $P_{ME}$  is the power of main engine and for the purpose of EEXI calculation, its value is 75% of the maximum continuous rating of installed engines onboard.  $SFC$  and  $CF$  are specific fuel consumption and CO<sub>2</sub> conversion factor corresponding to the main engine (ME) or auxiliary engine (AE).  $P_{AE}$  is the auxiliary engines power, in case of unavailability of electric power table like the current case study, its value can be evaluated as shown in Eq. (26) [55].

$$P_{AE} = 0.866 * GT^{0.732} \tag{26}$$

Moreover,  $P_{AE,eff}$  is the saving in auxiliary power resulting from the installation of innovative energy efficiency technologies such as the installation of WHR systems, and  $f_{eff}$  is the availability factor which should be equal to 1 if the installed technology can be used at any time [56].  $V_R$  is the reference ship speed for the purpose of EEXI calculation, it can be evaluated as shown in the guidelines [55].  $f_j$  and  $f_c$

are the correction factors for RO-RO passenger ships, their values can be calculated as shown in Eq. (27–28) [55].

$$f_j = \frac{1}{F_{nl}^\alpha * (L_{pp}/B)^\beta * (B/d)^\gamma * (L_{pp}/\nabla^{1/3})^\delta} \quad (27)$$

$$f_c = \left( \frac{DWT/GT}{0.25} \right)^{-0.8} \quad (28)$$

where  $L_{pp}$ ,  $B$ ,  $d$ ,  $\nabla$  are length, breadth, depth, and underwater volume of the case study, respectively. The exponents  $\alpha$ ,  $\beta$ ,  $\gamma$ , and  $\delta$  are 2.5, 0.75, 0.75, and 1, respectively [55].

## Performance evaluation assumptions

The parametric analysis is achieved to study the effect of changing main system's parameters on the performance from thermodynamic, economic, and technical perspectives. The condenser pressure is recommended to be equal to or more than 1 bar to prevent the leakage of air into the WHR system. Additionally, the integrated WHR system model in this work is based on the following assumptions: (1) pumps and turbines are presumed to be adiabatic equipment operating with a suitable range of isentropic efficiencies; (2) changes of kinetic and potential energy and exergy are considered to be insignificant; (3) the drop in pressure throughout the piping system is ignored; (4) the pinch point temperature is assumed to be 5 K; and (5) the systems are operating under steady-state conditions.

The utilization of the WHR system for maritime applications has some limitations that reduce the number of variables especially when the ORC is implemented as a WHR system. First, the temperature of the heat source is restricted to a specific range based on the main engine used onboard and the value of its load factor. For example, the engine emits exhaust gas at a temperature ranging from 300 to 550 °C, as well as the cooling water temperature ranges between 80 and 100 °C. Secondly, seawater is used as cooling medium in the ORC condenser whose average temperature value is around 25 °C, and the outlet temperature is set at 35 °C to prevent tube corrosion.

The engine is considered to run at rated conditions as shown in Fig. 1 since the study's research aims to optimize the settings for TEG–ORC utilization in heat recovery. The main design point parameters for the simulation inside MATLAB model are described in Table 4.

The ORC mediums are divided into dry, wet, and isentropic fluids. The difference between these types is based on their results in the expansion processes which depend on the slope of the saturated vapor curve in temperature-entropy diagrams [57]. When the expansion process ends in the

**Table 4** Design point parameters and constraints for TEG–ORC system

Parameter	Value
Exhaust gas mass flow rate/kg s <sup>-1</sup>	22.2
Exhaust gas temperature/K	609
Jacket water cooling temperature/K	353
Pump / turbine efficiency/%	80%
Temperature difference in preheater/K	60
Pinch point temperature difference/K	5
Cold end temperature difference of condenser and TEG/K	5

**Table 5** Thermo-environmental properties of the working fluid [59, 60, 62]

Property	Value
Chemical formula	CHCl <sub>2</sub> CF <sub>3</sub>
Boiling point/K	300.9
Molecular mass/g mol <sup>-1</sup>	152.9
Density/kg m <sup>-3</sup>	550
Critical temperature/K	456.8
Decomposition temperature/K	600
Vapor/liquid specific heat/kJ kg <sup>-1</sup> K <sup>-1</sup>	0.72 / 0.965
Ozone depletion potential	0.012
Global warming potential	120

two-phase area at the turbine's intake, for instance, because the slope of the saturated vapor curve for wet fluids is negative, the turbine's blades may be damaged, and its efficiency may be reduced. On the other hand, the expansion process ends in the superheated region because the slope is positive for dry working fluids. Furthermore, the cycle efficiency by using dry working mediums is higher than that one by using isentropic fluids [58].

In the current paper, the dry working fluid R123 has been selected to be the working fluid in ORC cycle. This selection has been done based on its features such as low cost, availability, low ozone depletion, excellent environmental properties, and thermal stability. Moreover, it complies with safety requirements as recommended by IMO as shown in Table 5 [59, 60] in terms of autoignition temperature, flammability, flashpoint temperature, and toxicity. Moreover, dry liquids such as R123 have a decomposition temperature of 600 K, so it will increase the ability to operate at high temperatures without liquid decomposition such as occurs in exhaust gas recovery from main engines. The comparative thermodynamic analysis between several working fluids conducted by Aghahosseini and Dincer [61], its results showed that R123 is displayed the optimal potential to improve the ORC cycle efficiency and hence possessed the lowest irreversibility.



## Results and discussion

For maritime applications, the net output power from the combined waste heat recovery is more crucial than the output power of every component in the integrated system. Moreover, the size and mass of the proposed integrated system must be controlled to eliminate the high size and mass that cannot be fitted inside the engine room of the ship. Therefore, the volumetric expansion ratio of the turbine must be well calculated to control the size of the system.

### Effect of working fluid specification on TEG performance

By using the set data in Table 4 which describe the input data of the model, the performance of TEG can be predicted. The exhaust gas from the main engine is considered the heat source of the TEG unit, while the working fluid is considered the heat sink. The heat source has a constant temperature and mass flow rate equal to 609 K and 22.2 kg s<sup>-1</sup>, respectively. While the temperature and mass flow rate of the working fluid can differ to select the optimum point. In the current analysis, the value of the working fluid's mass flow rate will be changed between 0.4 kg s<sup>-1</sup> and 1.4 kg s<sup>-1</sup> with the temperature of 300, 304, 308, and 312 K. The pressure of the working fluid is kept constant at 40 bar. The performance of TEG in terms of output power and efficiency is shown in Fig. 5.

As shown in Fig. 5, the highest performance is determined by using working fluid with a high mass flow rate and lower temperature. The output power from the TEG is estimated to be 304 kW with efficiency of 6.84% when the mass flow rate and temperature of working fluid are 1.4 kg s<sup>-1</sup> and 300 K, respectively. On the other hand, the output power and efficiency are 221 kW and 5.7%, respectively, when the mass flow rate and temperature of the working fluid are set at 0.4 kg s<sup>-1</sup> and 312 K, respectively. Moreover, the output power of TEG at 300 K is increased from 236 to 304 kW with an increment in the efficiency from 5.88% to 6.84% when the mass flow rate is increased from 0.4 kg s<sup>-1</sup> to 1.4 kg s<sup>-1</sup>.

The performance results in Fig. 5 reveal an inverse relationship between the working fluid inlet temperature and the output power from the TEG unit. This prediction is considered logical and correct as the increment in mass flow rate and lowering of temperature leads to a lower mean temperature of the working fluid in the cold side of the TEG. Therefore, the performance of TEG is predicted to be enhanced since the difference in the mean temperature between the hot side and cold side became larger.

Furthermore, the working fluid specification influences the levelized power cost of the TEG which can be evaluated

by using Eq. (21). The results have been graphically presented in Fig. 6 for different mass flow rate cases and four sets of working fluid's temperature at the inlet of TEG cold side.

The economic results show that the lowest levelized power cost can be achieved by using the highest mass flow rate case and the lowest inlet temperature. The optimum levelized power cost equal to 239 € kW<sup>-1</sup> that is occur at mass flow rate of 1.4 kg s<sup>-1</sup> and working fluid's temperature equal to 300 K. This value is considered better than the achieved value by using a flow rate equal to 0.4 kg s<sup>-1</sup> by about 7.2% for the same working temperature.

### Effect of TEG scaling on combined WHR system performance

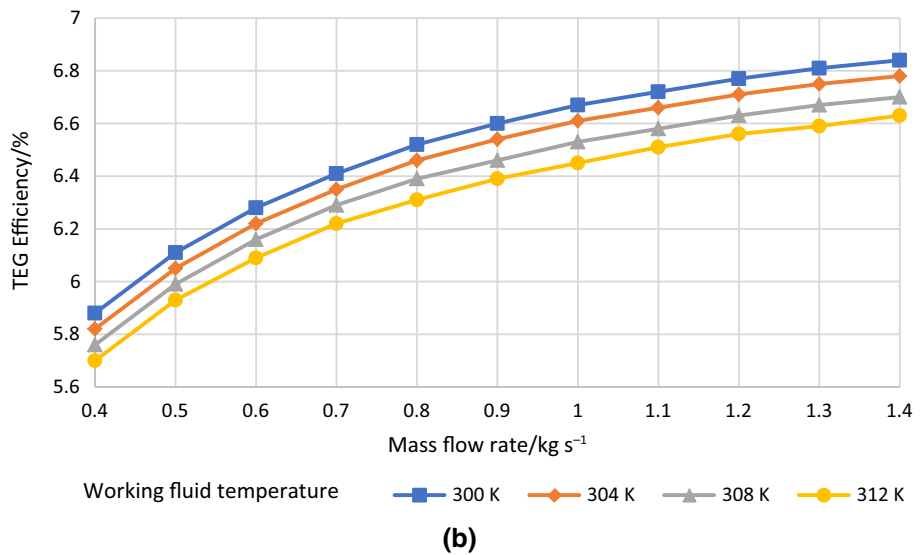
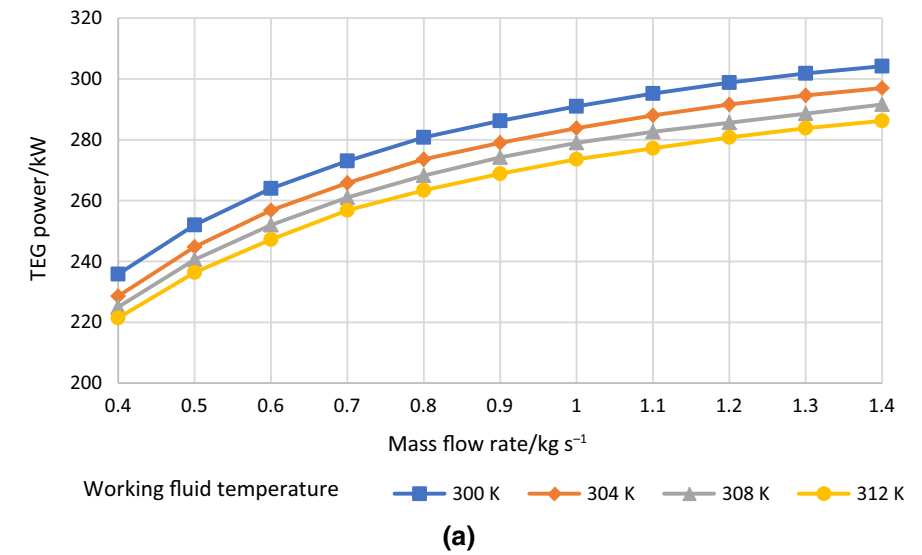
Furthermore, the effect of TEG scaling will be investigated to show the potential impact on the performance of the integrated WHR system. From the theoretical concept, the increasing of TEG scaling will lower the temperature of the flow stream at point B which enters the evaporator because more heat is predicted to be absorbed into TEG with the scaling increment. Therefore, different configuration and scales of TEG is proposed to be investigated at two different evaporation pressure, one for the subcritical (30 bar) and the other for the supercritical (55 bar). The TEG configuration effect can be managed by varying the temperature of stream flow at point B, which is controlled to be lowered from 600 K to about 430 K.

Figure 7 shows the power prediction of the TEG, pump, ORC turbine, and the combined WHR system at different temperatures and two evaporation pressures. The same data inputs that described in Table 4 are kept constant over the different configuration of TEG. The increment in temperature of point B as shown in Fig. 7 related to the lowering of TEG scaling as illustrated before.

As shown in Fig. 7a simulated at subcritical conditions, the TEG power reduces with the increase of temperature and lowering of the TEG scaling as TEG power reduces from 240 kW at approximately 430 K to about 45 kW at 600 K. While the power of the pump and ORC turbine are kept constant through the simulation at about 56 kW and 1226 kW, respectively. Therefore, the net power from the combined WHR system is about 1,410 kW at the lowest temperature (430 K) and reduces to 1,215 kW at the highest temperature (600 K).

Similarly, Fig. 7b which simulated the supercritical conditions proves the same trend occurred in the subcritical conditions. The TEG power decreases from 224 to 35 kW while keeping the power of the pump and ORC turbine constant at 119 kW and 1371 kW, respectively. Furthermore, the net power from the combined TEG–ORC system is predicted

**Fig. 5** Performance of TEG at different cases of working fluid's mass flow rate **a** output power and **b** efficiency



**Fig. 6** Levelized power cost of TEG at different cases of working fluid's mass flow rate

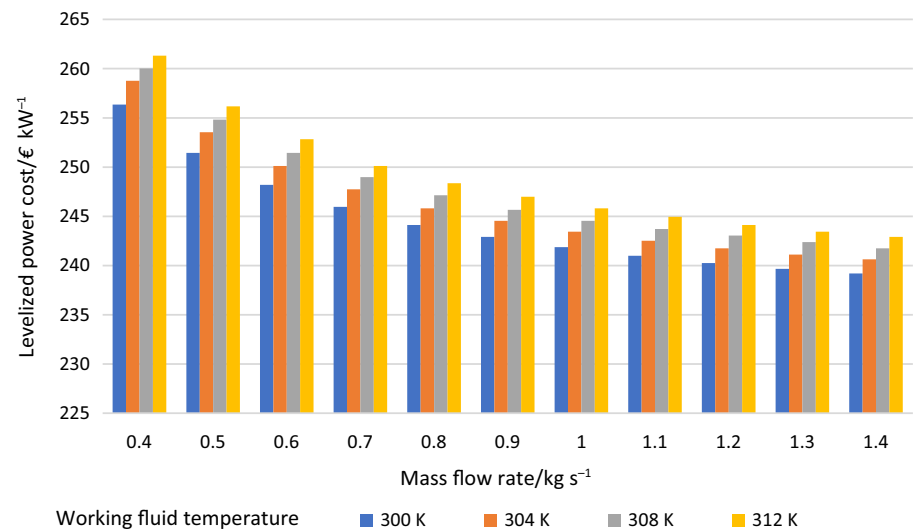
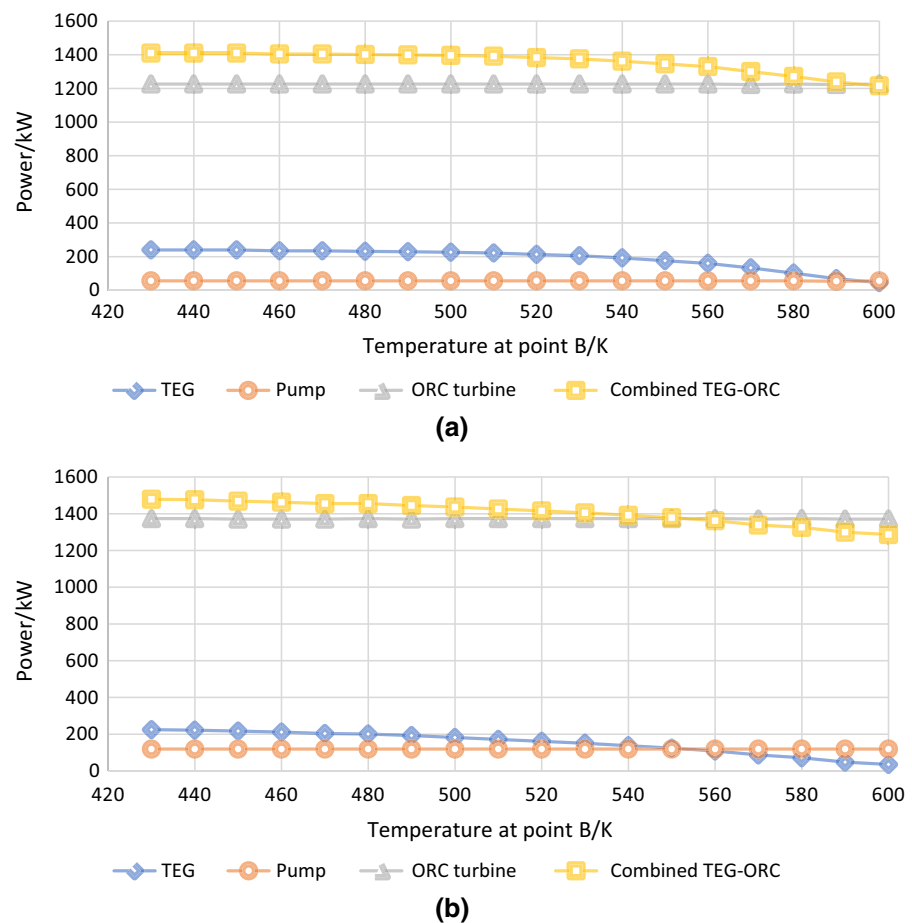


**Fig. 7** Effect of TEG scaling on the output power of different components in the proposed WHR system **a** subcritical at 30 bar and **b** supercritical at 55 bar



to decrease from 1,479 kW to 1,287 kW when rising the temperature from 430 to 600 K.

The results prove the efficient performance of the proposed WHR system under several conditions, particularly the lower range of temperature that relates to the increment of TEG scaling. Especially, the exhaust gas entering the evaporator with a lower temperature helps to prevent the resolving of the working fluid.

The integration of the proposed WHR system with the marine engine influences total efficiency; moreover, the amount of fuel saving is considered one of the potential benefits of using the TEG–ORC system. Therefore, Fig. 8 investigates the potential benefits of the proposed WHR system on the efficiency of marine diesel engine and fuel saving at subcritical and supercritical conditions.

The results presented in Fig. 8 show that the highest efficiency improvement occurs when using high scaling of TEG with lower temperature at the inlet of the evaporator. In subcritical conditions, the efficiency improvement rate reduces from 5.44% to 4.61% coinciding with the increase in the temperature of exhaust gas entering the evaporator from 430 to 600 K. A similar trend is observed in the supercritical conditions as the efficiency reduces with the

increase in temperature. The efficiency improvement is about 5.7% at 430 K, while it reports 4.93% by increasing the temperature to 600 K.

Furthermore, Fig. 8 shows the effect of TEG scaling on the fuel saving amount at subcritical conditions, it records the highest saving of about 244 kg hour<sup>-1</sup> at 430 K, while the lowest saving of about 207 kg hour<sup>-1</sup> at 600 K. While these values increase to 256 kg hour<sup>-1</sup> and 221 kg hour<sup>-1</sup> by using supercritical conditions and coinciding with temperatures of 430 K and 600 K, respectively.

From the economical point of view, the influence of TEG scaling can be assessed by calculating the levelized power cost and the discounted payback time as shown in Fig. 9.

As expected, the TEG scaling has a direct impact on levelized power cost of TEG as the increasing of scaling and lowering the temperature at point (B) from 600 to 430 K at subcritical conditions reduces the levelized power cost from 791 € kW<sup>-1</sup> to 466 € kW<sup>-1</sup>, while the LPC reduces from 915 € kW<sup>-1</sup> to 480 € kW<sup>-1</sup> at supercritical conditions. The similar trend is observed when calculating the discounted payback time of investment in TEG–ORC system as shown in Fig. 9. The discounted payback time at 600 K and 30 bar is about 3.1 years, while it lowers to about 3 years with an

**Fig. 8** Comparison of efficiency improvement and fuel saving from the WHR system at subcritical and supercritical conditions

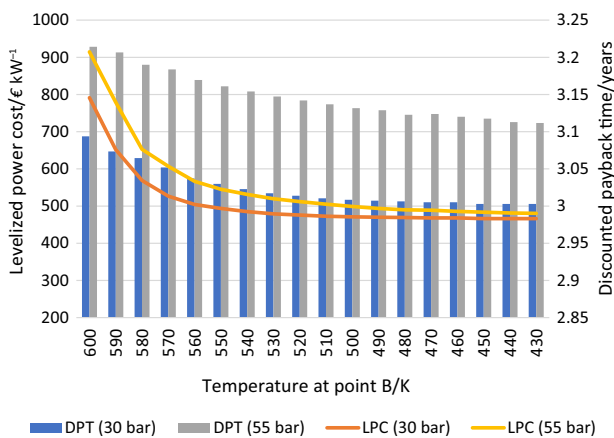
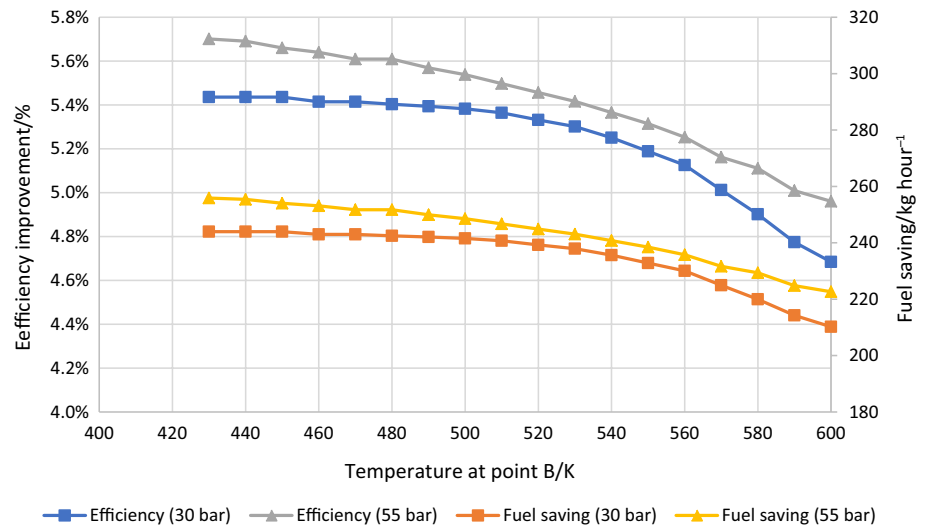


**Fig. 9** Effect of TEG scaling on levelized power cost and payback time of TEG–ORC system

improvement equal to 3% when the temperature reduces to 430 K. Also, at supercritical conditions, the DPT improves by about 3.2% when the temperature reduces from 600 to 430 K.

### Effect of temperature and evaporation pressure on the ORC performance

The ORC is composed of turbine, condenser, pump, and evaporator. The highest temperature occurs on the inlet of the turbine and the output of the evaporator (point 5) as shown in Fig. 2. Therefore, the temperature at this point can be utilized to investigate the performance of the system under different evaporation pressures. The condensation temperature is kept constant at 300 K with the assumption of operating the ORC system alone without its integration with TEG to investigate the effect of the maximum temperature

on the system performance. Figure 10 shows the impact of evaporation pressure and maximum temperature ( $T_5$ ) on the ORC performance in terms of the specific power (net output power per unit of working fluid mass flow rate, measured in  $\text{kW kg}^{-1} \text{s}$ ) and the total net output power measured in kW.

As shown in Fig. 10, there is a direct relationship between the temperature and the specific power, the specific power increases gradually with the increment in the maximum temperature. This gives evidence of the ability of the selected working fluid to convert heat to power in parallel with the increase in the maximum temperature. On the other hand, the output power has a different impact based on the type of conditions whether it is subcritical conditions or supercritical conditions in terms of the evaporation pressure. For example, when the evaporation pressure is 20 bar that describes working on subcritical conditions, the power is increased and then reduced slightly with the rising of the maximum temperature. The maximum achievable net output power is 288 kW at 465 K, while the minimum achievable out power is 277 kW at 590 K. On the other hand, the net out power increases with the rising of maximum temperature when operating at supercritical conditions. For an evaporation pressure of 80 bar, the output power is increased from 300 kW to about 382 kW with an improvement equal to 27% when raising the maximum temperature from 485 to 590K.

Furthermore, the effect of overheating and different evaporation pressures on the volumetric expansion ratio is analyzed as shown in Fig. 11. The results revealed that volumetric expansion ratio reduces when the maximum temperature rises at different evaporation pressures. For example, the volumetric expansion ratio reduces from 33 to about 21.4 when the temperature of working fluid at the turbine inlet increases from 445 to 600 K at 30 bar as an evaporation pressure. For supercritical conditions at 50 bar as an evaporation pressure, the expansion ratio reduces from 80 at 475

**Fig. 10** Effect of temperature and evaporation pressure on ORC performance

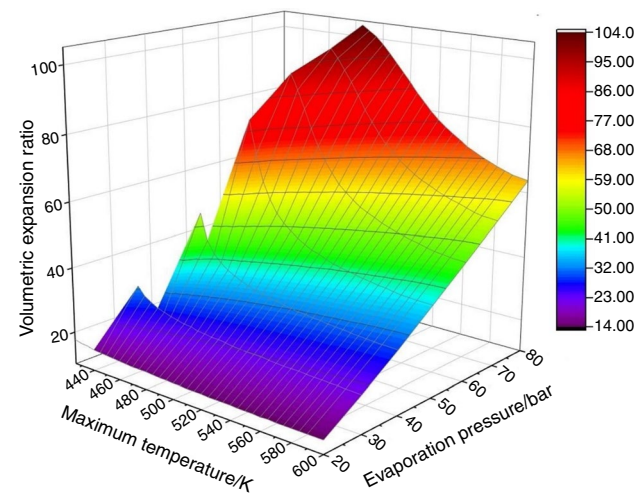
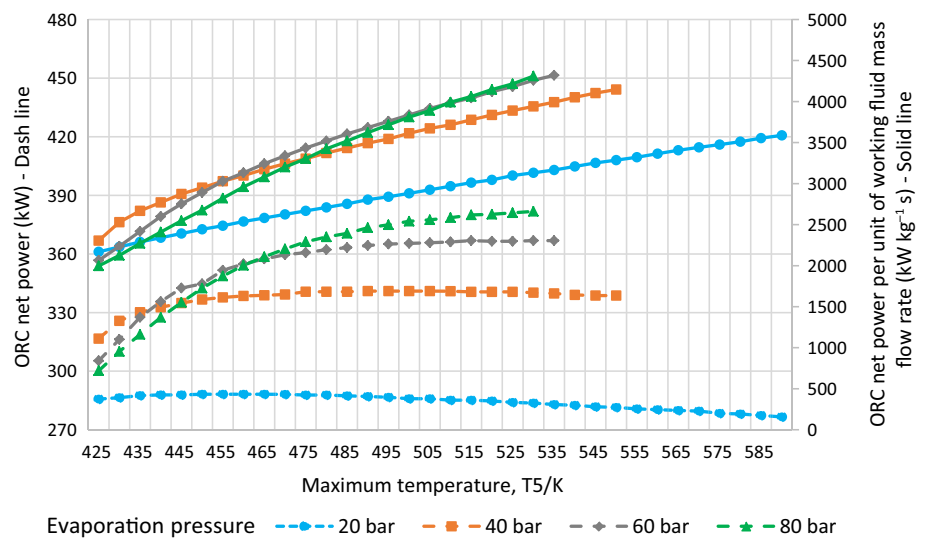


**Fig. 11** Effect of temperature and evaporation pressure on volumetric expansion ratio

K to about 37.7 at 600 K. These results prove the ability of R123 to recover waste heat and convert it into useful power at different conditions of temperatures at the turbine inlet, especially when it rises.

**Effect of recuperator addition on the performance**

To investigate the effect of recuperator addition to the system, four different cases will be studied at different evaporation pressures. The first two cases are based on using simple ORC and rcORC to recover the exhaust heat from the engine, while the other cases are based on the integrated systems of TEG–ORC and TEG–rcORC. The net power output has been calculated for all cases at different evaporation pressures as shown in Fig. 12.

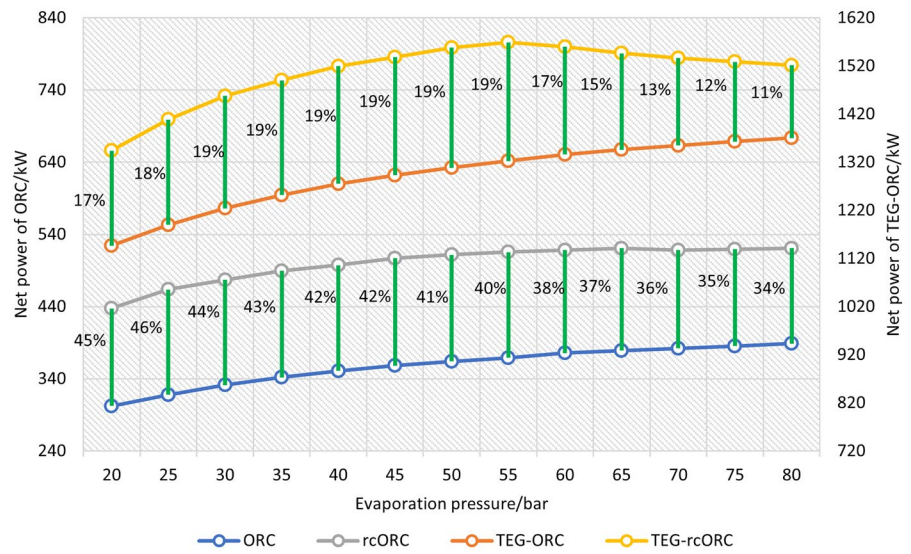
The results revealed that the addition of the recuperator to the ORC system and TEG–ORC system increases the net output power by a significant amount. For the ORC system only, the net power output enhances by increasing the evaporation pressure as it increases from 302 to 389 kW (+29% as an improvement) when the evaporator pressure is increased from 20 to 80 bar, respectively. While for the rcORC system, the net power output increases from 437 kW at 20 bar to 521 kW at 80 bar. The improvement in net power output of the ORC system from the installation of the recuperator has been presented as a green vertical line in Fig. 12, the improvement range is between 34 and 46%.

Likewise, for the TEG–ORC system, the net output power increases by adding the recuperator to the system, for example, the net output power corresponding to 55 bar is equal to 1569 kW, while it was 1322 kW without recuperator. Nevertheless, the improvement percentage achieved in the TEG–ORC system after the addition of the recuperator has been reduced to the range between 11 and 19%.

Furthermore, the results indicate that the integration between the TEG and ORC gives the opportunity to generate more power as shown at different evaporation pressures. However, the enhancement is significantly dependent on the evaporation pressure of the working fluid as the increasing trend is changed to be more gentle when reaching and exceeding the critical pressure. For example, the net output power of the TEG–ORC is enhanced by about 17%–19% when increasing the pressure from 20 to 55 bar, while the enhancement percentage is lowered to be between 17 and 11% with increasing pressure up from 55 bar. A similar trend has been observed in using ORC only with the recuperator as shown in Fig. 12.

From the economical point of view, Fig. 13 shows the effect of recuperator addition to the ORC system and

**Fig. 12** The impact of recuperator addition to the ORC system only and combined TEG–ORC system at different evaporation pressures



TEG–ORC system on the annual saving in operational expenses which has been calculated based on Eq. (22).

There is a significant improvement in the annual saving of expenses (fuel expenses and CO<sub>2</sub> taxes) resulting from the addition of a recuperator because of the increased generated power. The annual saving achieved in the proposed TEG–ORC system is in the range of 770k € – 920k € at different evaporation pressure between 20 and 80 bar, while this range rises to 903k € – 1.05 M€ when the recuperator is integrated to TEG–ORC system. The optimum point in terms of annual saving of expenses is achieved by using an evaporation pressure equal to 55 bar in the fourth case (TEG–rcORC) as the annual saving in expenses equals 1.05 M€.

Furthermore, the levelized power cost has been calculated to examine the influence of recuperator addition by using the discussed procedure in Sect. "Economic modeling of the combined system". The LPC has increased from 220.3

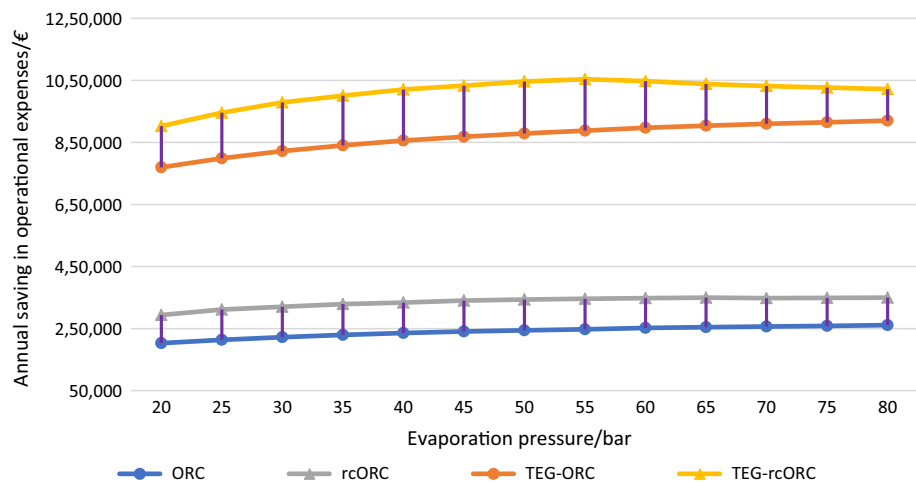
€ kW<sup>-1</sup> to 267.3 € kW<sup>-1</sup> when recuperator addition is done for ORC system only, while the LPC is increased by addition of recuperator to the TEG–ORC system from 233.2 € kW<sup>-1</sup> to 280.2 € kW<sup>-1</sup>. The effect of recuperator addition to the system can be assessed by evaluating the discounted payback time, and its results are shown in Fig. 14.

The results shown in Fig. 14 reveals the direct impact of recuperator addition to the two cases as the payback time increased from 3 years to 3.7 years for ORC system only, while the payback time increases from 3.2 years to 3.9 years for the integrated TEG–ORC system.

### Exergy analysis results

To assess the performance of TEG–ORC system with or without the addition of a recuperator, the second law of thermodynamic can be considered since it offers more insightful

**Fig. 13** The annual saving in fuel costs and CO<sub>2</sub> taxes calculated at different evaporation pressures



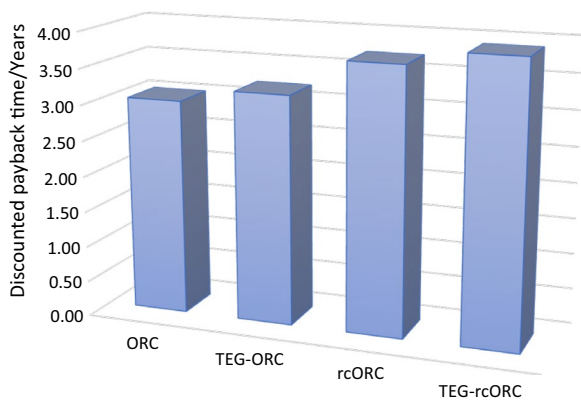


**Fig. 14** Discounted payback time expressed in years for recuperator addition to ORC and combined TEG–ORC systems

analysis. Therefore, the exergy analysis of the proposed system with and without recuperator is done under two different conditions, one for subcritical conditions at evaporation pressure equal to 30 bar and the other based on supercritical conditions at 55 bar. The results of main parameters such as volumetric expansion ratio, mass flow rate of working fluid, net output power, and efficiency improvement over the main engine’s efficiency are shown in Table 6.

As shown in Table 6, the volumetric expansion is increased with the addition of recuperator to the proposed system as it increases from 30 to 31.1 at subcritical conditions, while it increases from 50.4 to 63.7 at supercritical conditions. It reflects that working in subcritical conditions is more beneficial than in supercritical conditions in terms of the size and mass of the turbine that based on the volumetric expansion ratio.

Moreover, the net output power of the proposed system is evaluated at 30 bar, and its value is 1,224 kW and 1,458 kW for TEG–ORC system and TEG–rcORC system, respectively, while these values are increased when operating at supercritical conditions to about 1,322 kW and 1,569 kW. The net output power from the TEG–ORC system is added to the rated power from the main engine to evaluate

the total energy efficiency as shown in Table 6. The efficiency improvement after the addition of the proposed system at 30 bar is 4.7%, and 5.6% for TEG–ORC system and TEG–rcORC system, respectively. Also, the addition of a recuperator to the TEG–ORC system rises the efficiency improvement from 5.1% to 6.1% at 55 bar, respectively.

The exergy losses of each component in the proposed system are evaluated while modeling it with and without recuperator. For example, the exergy losses at subcritical conditions for TEG–rcORC case study is 300.6, 154.2, 22.8, 525.6, and 58.2 kW for turbine, condenser, pump, TEG, and recuperator, respectively, while the exergy losses of the same system components at supercritical conditions are 356.4, 152.4, 33, 964.2, and 42 kW, respectively. Figure 15 shows the contribution percentage of each component to the total exergy losses for four case studies that investigate the TEG–ORC system and TEG–rcORC system at 30 bar and 55 bar. The total exergy losses are 1825 kW, and 1742 kW for TEG–ORC system at 30 bar and 55 bar, respectively, while the total exergy losses are 1699 kW, and 1660 kW for TEG–rcORC system at 30 bar and 55 bar, respectively.

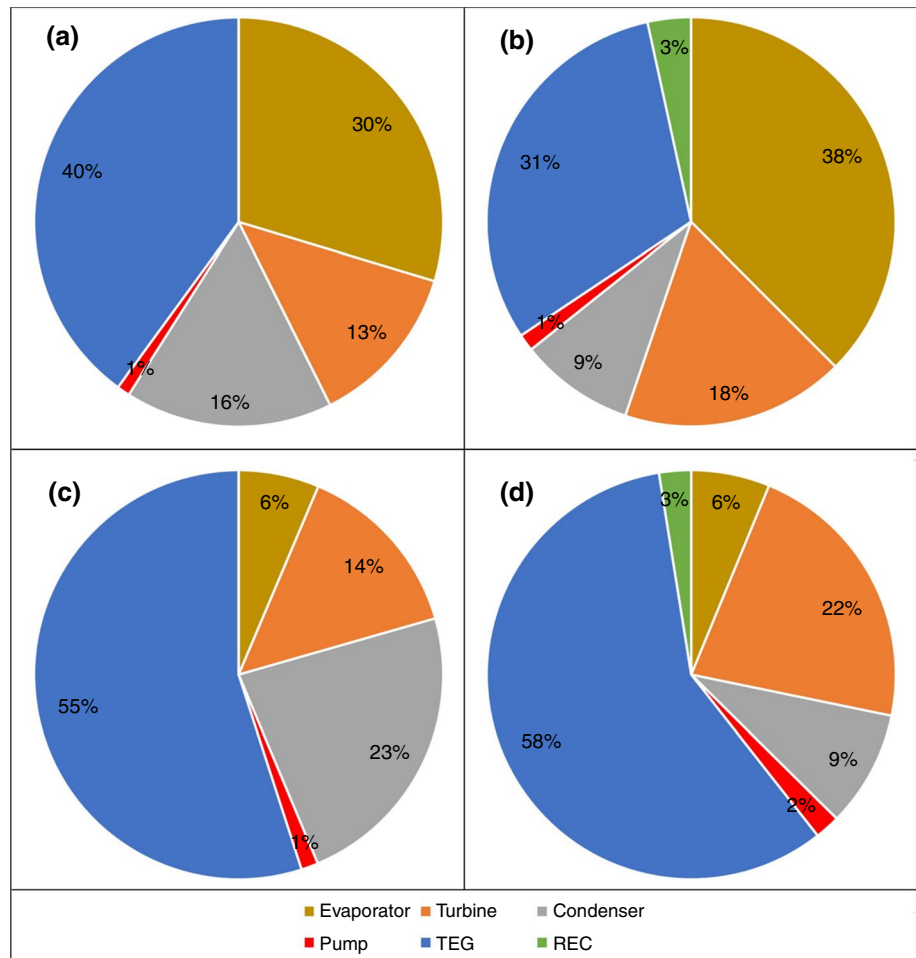
In all cases, the TEG has the largest contribution in the total exergy losses of the system by about 40%, 31%, 55%, and 58% for cases a, b, c, and d, respectively. While the pump contributes by the lowest percentage in the total exergy losses of all cases by about 1–2%, it is followed by the recuperator for cases of TEG–rcORC system at 30 bar and 55 bar. Moreover, the results indicate that contribution of evaporator in exergy losses of the TEG–ORC system and TEG–rcORC system at subcritical conditions is more than its contribution in supercritical conditions. However, the exergy losses’ contribution from TEG at subcritical conditions is lower than its contribution in supercritical conditions. The result implies that the system would recuperate a sizable quantity of power once TEG technology achieves progress in more energy conversion efficiency.

The exergy efficiency of the TEG–ORC system is 40.2% and 43.2% when evaporator pressure is 30 bar and 55 bar, respectively, while the exergy efficiency improves to 46.2% and 48.6% through the addition of the recuperator to the system at 30 bar and 55 bar, respectively. This improvement

**Table 6** Results of main parameters for TEG–ORC system and TEG–rcORC system at subcritical and supercritical conditions

Parameter	Subcritical conditions		Supercritical conditions	
	TEG–ORC	TEG–rcORC	TEG–ORC	TEG–rcORC
Volumetric expansion ratio	30	31.1	50.4	63.7
Turbine power/kW	1098	1302	1224	1398
Pump power/kW	60	74	91	128
TEG power/kW	186	230	189	299
Net output power/kW	1224	1458	1322	1569
Engine + WHR energy efficiency/%	51.9%	52.8%	52.3%	53.2%
Efficiency improvement/%	4.7%	5.6%	5.1%	6.1%
Mass flow rate of working fluid/kg s <sup>-1</sup>	20.52	25.38	17.82	25.2

**Fig. 15** Contribution percentage of each component in the total exergy losses for (a) TEG–ORC system at 30 bar, (b) TEG–rcORC system at 30 bar, (c) TEG–ORC system at 55 bar, and (d) TEG–rcORC at 55 bar



is due to the ability of the recuperator in recovering a greater portion of the working medium's energy that exhaust from the turbine which results in less exergy loss in the condenser. Therefore, the results demonstrate the potential benefits of adding a recuperator to the TEG–ORC system in terms of improving the exergy efficiency and generating more power.

### Technical analysis results

This section shows the results of the technical analysis and the effect of the installation the proposed WHR system onboard the case study. The technical regulatory indicator recommended by IMO to the existing ships in-service called the EEXI has been evaluated for the case study. Figure 16 shows the results of the reference line and the required EEXI for passenger ships that have a DWT of up to 12,000 tons, these values have been calculated by using the formula in Eq. (24). For the case study which has a DWT of 6,515 tons, the value of EEXI on reference line is  $26.5 \text{ g-CO}_2 \text{ ton}^{-1} \text{ nm}^{-1}$ , while the required EEXI is  $25.2 \text{ g-CO}_2 \text{ ton}^{-1} \text{ nm}^{-1}$ .

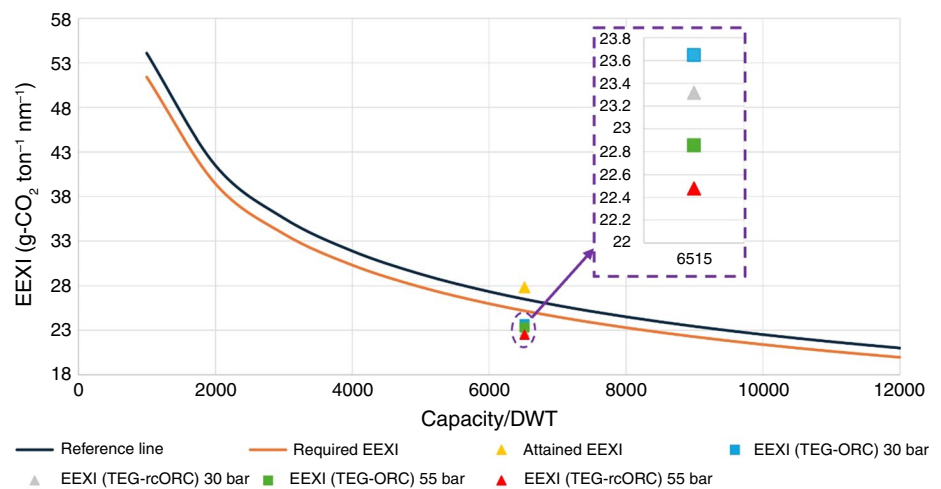
As mentioned before in Sect. "Technical analysis approach", the attained EEXI must be compared with the

required EEXI to assess the energy efficiency level of the ship and its compliance with the IMO requirements. By using the formulas in Eq. (25), the attained EEXI of the ship before the addition of the WHR system is  $27.8 \text{ g-CO}_2 \text{ ton}^{-1} \text{ nm}^{-1}$ . By comparing this value with the required one, it is observed that the attained EEXI is higher than the required one by 10.4% which proves its unfulfillment with IMO rules. Therefore, the WHR installation is mandatory for this case study to reduce the attained EEXI to an acceptable level.

The attained EEXI has been recalculated by considering the net output power from the proposed WHR system in different cases as mentioned in Table 6. The results show that attained EEXI is  $23.65 \text{ g-CO}_2 \text{ ton}^{-1} \text{ nm}^{-1}$  (lower than the required EEXI by 6%) by using the TEG–ORC system at subcritical conditions (30 bar). Also, by using TEG–rcORC system, the attained EEXI is  $22.85 \text{ g-CO}_2 \text{ ton}^{-1} \text{ nm}^{-1}$  (9% lower than the required EEXI). At supercritical conditions (55 bar), the attained EEXI is improved to be  $23.32 \text{ g-CO}_2 \text{ ton}^{-1} \text{ nm}^{-1}$  and  $22.47 \text{ g-CO}_2 \text{ ton}^{-1} \text{ nm}^{-1}$  corresponding to TEG–ORC system and TEG–rcORC system, respectively. In this way, the attained EEXI in the case of using the TEG–ORC system or TEG–rcORC system at 55 bar is lower



**Fig. 16** Required EEXI and attained EEXI values at different design cases



than the required EEXI by 7% or 11%, respectively. These results prove that the installation of the TEG–ORC system enhances the energy efficiency of ships and facilitates the fulfillment of current and future IMO requirements.

## Conclusions

In this paper, a combined WHR system formed by TEG and ORC was applied to recover the waste heat that exists in the exhaust gases and jacket cooling water from a marine diesel engine installed onboard a passenger ship. The performance of the system has been investigated with emphasis on energy, exergy, economic, and technical analysis. The TEG–ORC system consists of TEG, preheater, turbine, condenser, and pump, while the second scenario (TEG–rcORC) proposed the installation of a recuperator between ORC turbine and TEG. The parametric and techno-economic analysis of the combined TEG–ORC system has been modeled and developed by using MATLAB. The dry fluid (R123) has been employed as a working medium as it can operate at high temperatures without decomposition and is considered an eco-friendly fluid thanks to its lower global warming potential. The effects of working fluid specifications on TEG performance, TEG scaling, temperature, recuperator addition, and evaporator pressure are investigated based on the evaluation assumptions and input parameters from the diesel engine. The main findings from the parametric analysis are summarized as follows:

- Using a working fluid with a high mass flow rate and low inlet temperature results in the best performance for TEG. When the working fluid's mass flow rate and temperature are  $1.4 \text{ kg s}^{-1}$  and  $300 \text{ K}$ , respectively, the net output power from the TEG is  $304 \text{ kW}$  with an efficiency

of 6.84%, and its levelized power cost is equal to  $239 \text{ € kW}^{-1}$ .

- The results indicate that the increasing of TEG scaling leads to better performance of the combined WHR system. By using high TEG scaling at subcritical conditions (30 bar), the net output power and levelized power cost of the combined WHR system is  $1,410 \text{ kW}$  and  $466 \text{ € kW}^{-1}$ , respectively. Moreover, the efficiency of the integrated power system with combined WHR system is improved by about 5.4% with achieving fuel saving equal to  $244 \text{ kg hour}^{-1}$ .
- The findings demonstrate the ability of the working fluid (R123) to collect waste heat and transform it into usable power under a variety of temperature circumstances at the turbine inlet, particularly when the temperature is rising. For example, under supercritical conditions (80 bar), the ORC's output power is increased from  $300 \text{ kW}$  to about  $382 \text{ kW}$  with an improvement equal to 27% when raising the maximum temperature from  $485$  to  $590 \text{ K}$ . Furthermore, the volumetric expansion ratio reduces from 104 to about 64 when rising the temperature from  $485$  to  $590 \text{ K}$ .
- The results revealed that the addition of the recuperator to the combined WHR system enhances thermo-economic performance by a significant amount. For example, at evaporation pressure of 55 bar, the net output power is enhanced by about 19% from  $1322 \text{ kW}$  without a recuperator to  $1569 \text{ kW}$  by adding a recuperator, moreover, the exergy efficiency of TEG–ORC system is enhanced from 43.2% to 48.6% by the addition of recuperator which improve the integrated thermodynamic efficiency of the power system (engine + WHR system) from 52.3% to 53.2%. Therefore, the annual saving in operational expenses is enhanced to achieve up to  $1.05 \text{ M€}$  as savings by adding the recuperator to the combined WHR system. While the LPC is increased

by the addition of a recuperator to the TEG–ORC system from 233.2 € kW<sup>-1</sup> to 280.2 € kW<sup>-1</sup> with an increase in the payback time from 3.2 years to 3.9 years.

- The technical analysis results revealed that the installation of TEG–ORC system will facilitate the fulfillment of EEXI requirements as recommended by IMO. The findings prove that the attained EEXI in the case of subcritical or supercritical conditions is lower than the required EEXI by 6–11%.

The current paper showed that the TEG–ORC system is appropriate for recovering waste heat from marine diesel engines at different parametric conditions while achieving optimum performance at supercritical conditions. Moreover, the thermo-economic performance is significantly improved by the inclusion of the recuperator in the system. Furthermore, the installation of this integration TEG–ORC system onboard system is recommended to facilitate compliance with current and future IMO regulations especially the EEXI, and the results prove its economic benefit in terms of reduction in fuel expenses and CO<sub>2</sub> taxes.

**Authors' contributions** Ahmed G. Elkafas performed conceptualization, methodology, software, data curation, writing—original draft preparation, formal analysis, visualization, investigation, supervision, validation, and writing—reviewing, and editing.

**Funding** This research did not receive any specific grant from funding agencies in the public, commercial, or not-for-profit sectors.

## Declarations

**Conflict of interest** The authors declare that they have no conflict of interest.

**Ethics approval** Not applicable.

**Consent to Participate** Not applicable.

**Consent for publication** Not applicable.

## References

1. IMO. Fourth IMO Greenhouse Gas Study. International Maritime Organization: London, UK 2021:197–212. <https://www.imo.org/en/ourwork/Environment/Pages/Fourth-IMO-Greenhouse-Gas-Study-2020.aspx>. Accessed 15 Mar 2024.
2. IMO. Report of fuel oil consumption data submitted to the IMO Ship Fuel Oil Consumption Database in GISIS (Reporting year: 2021). 2022. <https://www.imo.org/en/ourwork/environment/pages/data-collection-system.aspx>. Accessed 15 Mar 2024.
3. IMO. Initial IMO strategy on reduction of GHG emissions from ships. London, UK: 2018. <https://www.imo.org/en/OurWork/Environment/Pages/IMO-Strategy-on-reduction-of-GHG-emissions-from-ships.aspx>. Accessed 15 Mar 2024.
4. IMO. 2023 IMO strategy on reduction of GHG emissions from ships. RESOLUTION MEPC377(80) 2023;July:1–18. [www.imo.org/en/OurWork/Environment/Pages/2023-IMO-Strategy-on-Reduction-of-GHG-Emissions-from-Ships.aspx](https://www.imo.org/en/OurWork/Environment/Pages/2023-IMO-Strategy-on-Reduction-of-GHG-Emissions-from-Ships.aspx). Accessed 15 Mar 2024.
5. European Commission. Fourth Annual Report from the European Commission on CO<sub>2</sub> Emissions from Maritime Transport (period 2018–2021). Brussels: 2023. [https://climate.ec.europa.eu/system/files/2023-03/swd\\_2023\\_54\\_en.pdf](https://climate.ec.europa.eu/system/files/2023-03/swd_2023_54_en.pdf). Accessed 15 Mar 2024.
6. European Commission. Reducing emissions from the shipping sector. Transport Emissions 2023. [https://climate.ec.europa.eu/eu-action/transport-emissions/reducing-emissions-shipping-sector\\_en#studies](https://climate.ec.europa.eu/eu-action/transport-emissions/reducing-emissions-shipping-sector_en#studies). Accessed 15 Mar 2024.
7. RICARDO. Technological, Operational and Energy Pathways for Maritime Transport to Reduce Emissions Towards 2050 2022. <https://www.concawe.eu/publication/technological-operational-and-energy-pathways-for-maritime-transport-to-reduce-emissions-towards-2050-concawe-review-31-1/>. Accessed 23 Aug 2023.
8. Bouman EA, Lindstad E, Riialand AI, Strømman AH. State-of-the-art technologies, measures, and potential for reducing GHG emissions from shipping – A review. *Transp Res D Transp Environ*. 2017;52:408–21. <https://doi.org/10.1016/j.trd.2017.03.022>.
9. Elkafas AG. Advanced operational measure for reducing fuel consumption onboard ships. *Environ Sci Pollut Res*. 2022. <https://doi.org/10.1007/s11356-022-22116-7>.
10. Geertsma RD, Negenborn RR, Visser K, Hopman JJ. Design and control of hybrid power and propulsion systems for smart ships: a review of developments. *Appl Energy*. 2017;194:30–54. <https://doi.org/10.1016/j.apenergy.2017.02.060>.
11. MAN Diesel & Turbo. Waste Heat Recovery System (WHRS) for Reduction of Fuel Consumption, Emissions and EEDI. 2016.
12. Singh DV, Pedersen E. A review of waste heat recovery technologies for maritime applications. *Energy Convers Manag*. 2016;111:315–28. <https://doi.org/10.1016/j.enconman.2015.12.073>.
13. Díaz-Secades LA, González R, Rivera N, Montañés E, Quevedo JR. Waste heat recovery system for marine engines optimized through a preference learning rank function embedded into a Bayesian optimizer. *Ocean Eng*. 2023;281:114747. <https://doi.org/10.1016/j.oceaneng.2023.114747>.
14. Shu G, Liang Y, Wei H, Tian H, Zhao J, Liu L. A review of waste heat recovery on two-stroke IC engine aboard ships. *Renew Sustain Energy Rev*. 2013;19:385–401. <https://doi.org/10.1016/j.rser.2012.11.034>.
15. Palomba V, Dino GE, Ghirlando R, Micallef C, Frazzica A. Decarbonising the shipping sector: a critical analysis on the application of waste heat for refrigeration in fishing vessels. *Appl Sci (Switzerland)*. 2019;9:5143. <https://doi.org/10.3390/app9235143>.
16. Xu X, Li Y, Yang S, Chen G. A review of fishing vessel refrigeration systems driven by exhaust heat from engines. *Appl Energy*. 2017;203:657–76. <https://doi.org/10.1016/j.apenergy.2017.06.019>.
17. Song J, Song Y, Gu C. Thermodynamic analysis and performance optimization of an Organic Rankine Cycle (ORC) waste heat recovery system for marine diesel engines. *Energy*. 2015;82:976–85. <https://doi.org/10.1016/j.energy.2015.01.108>.
18. Baldi F, Larsen U, Gabriellii C. Comparison of different procedures for the optimisation of a combined Diesel engine and organic Rankine cycle system based on ship operational profile. *Ocean Eng*. 2015;110:85–93. <https://doi.org/10.1016/j.oceaneng.2015.09.037>.
19. Mondejar ME, Andreassen JG, Pierobon L, Larsen U, Thern M, Haglind F. A review of the use of organic Rankine cycle power systems for maritime applications. *Renew Sustain Energy Rev*. 2018;91:126–51. <https://doi.org/10.1016/j.rser.2018.03.074>.

20. Lion S, Taccani R, Vlaskos I, Scrocco P, Vouvakos X, Kaiktsis L. Thermodynamic analysis of waste heat recovery using Organic Rankine Cycle (ORC) for a two-stroke low speed marine Diesel engine in IMO Tier II and Tier III operation. *Energy*. 2019;183:48–60. <https://doi.org/10.1016/j.energy.2019.06.123>.
21. Casisi M, Pinamonti P, Reini M. Increasing the energy efficiency of an internal combustion engine for ship propulsion with bottom ORCS. *Appl Sci (Switzerland)*. 2020;10:1–18. <https://doi.org/10.3390/app10196919>.
22. Bayraktar M. Investigation of alternative fuelled marine diesel engines and waste heat recovery system utilization on the oil tanker for upcoming regulations and carbon tax. *Ocean Eng*. 2023;287:115831. <https://doi.org/10.1016/j.oceaneng.2023.115831>.
23. Jia X, Fan S, Zhang Z, Wang H. Performance assessment of thermoelectric generators with application on aerodynamic heat recovery. *Micromachines (Basel)*. 2021;12:1399. <https://doi.org/10.3390/mi12111399>.
24. Albatati F, Attar A. Analytical and experimental study of thermoelectric generator (Teg) system for automotive exhaust waste heat recovery. *Energies (Basel)*. 2021;14:204. <https://doi.org/10.3390/en14010204>.
25. von Lukowicz M, Abbe E, Schmiel T, Tajmar M. Thermoelectric generators on satellites—an approach for waste heat recovery in space. *Energies (Basel)*. 2016;9:541. <https://doi.org/10.3390/en9070541>.
26. Uyanık T, Ejder E, Arslanoğlu Y, Yalman Y, Terriche Y, Su CL, et al. Thermoelectric generators as an alternative energy source in shipboard microgrids. *Energies (Basel)*. 2022;15:4248. <https://doi.org/10.3390/en15124248>.
27. Kristiansen NR, Nielsen HK. Potential for usage of thermoelectric generators on ships. *J Electron Mater*. 2010;39:1746–9. <https://doi.org/10.1007/s11664-010-1189-1>.
28. Georgopoulou CA, Dimopoulos GG, Kakalis NMP. A modular dynamic mathematical model of thermoelectric elements for marine applications. *Energy*. 2016;94:13–28. <https://doi.org/10.1016/j.energy.2015.10.130>.
29. Öksel C, Koç A. Modeling of a combined Kalina and organic rankine cycle system for waste heat recovery from biogas engine. *Sustainability*. 2022;14:7135. <https://doi.org/10.3390/su14127135>.
30. He M, Zhang X, Zeng K, Gao K. A combined thermodynamic cycle used for waste heat recovery of internal combustion engine. *Energy*. 2011;36:6821–9. <https://doi.org/10.1016/j.energy.2011.10.014>.
31. Qu J, Feng Y, Zhu Y, Zhou S, Zhang W. Design and thermodynamic analysis of a combined system including steam Rankine cycle, organic Rankine cycle, and power turbine for marine low-speed diesel engine waste heat recovery. *Energy Convers Manag*. 2021;245:114580. <https://doi.org/10.1016/j.enconman.2021.114580>.
32. MarineTraffic. Europa Palace ship. *Ships* 2023. [https://www.marinetraffic.com/en/ais/details/ships/shipid:407585/mmsi:247362700/imo:9198939/vessel:EUROPA\\_PALACE](https://www.marinetraffic.com/en/ais/details/ships/shipid:407585/mmsi:247362700/imo:9198939/vessel:EUROPA_PALACE). Accessed 22 Sep 2023.
33. Wikipedia contributors. MS Europa Palace. *Wikipedia, The Free Encyclopedia* 2023. [https://en.wikipedia.org/wiki/MS\\_Europa\\_Palace](https://en.wikipedia.org/wiki/MS_Europa_Palace). Accessed 22 Sep 2023.
34. Wartsila. Wartsila 46F product guide 2020. <https://www.wartsila.com/marine/products/engines-and-generating-sets/diesel-engines/wartsila-46f>. Accessed 22 Sep 2023.
35. Aliahmadi M, Moosavi A, Sadrhosseini H. Multi-objective optimization of regenerative ORC system integrated with thermoelectric generators for low-temperature waste heat recovery. *Energy Rep*. 2021;7:300–13. <https://doi.org/10.1016/j.egy.2020.12.035>.
36. Lou Y, Liu G, Romagnoli A, Ji D. TEG–ORC combined cycle for geothermal source with coaxial casing well. *Appl Therm Eng*. 2023;226:120223. <https://doi.org/10.1016/j.applthermaleng.2023.120223>.
37. Liu C, Li H, Ye W, Liu J, Wang H, Xu M, et al. Simulation research of TEG–ORC combined cycle for cascade recovery of vessel waste heat. *Int J Green Energy*. 2021;18:1173–84. <https://doi.org/10.1080/15435075.2021.1897824>.
38. Xu B, Rathod D, Yebi A, Filipi Z. A comparative analysis of real-time power optimization for organic Rankine cycle waste heat recovery systems. *Appl Therm Eng*. 2020;164:114442. <https://doi.org/10.1016/j.applthermaleng.2019.114442>.
39. Saadat-Targhi M, Khanmohammadi S. Energy and exergy analysis and multi-criteria optimization of an integrated city gate station with organic Rankine flash cycle and thermoelectric generator. *Appl Therm Eng*. 2019;149:312–24. <https://doi.org/10.1016/j.applthermaleng.2018.12.079>.
40. Zare V, Palideh V. Employing thermoelectric generator for power generation enhancement in a Kalina cycle driven by low-grade geothermal energy. *Appl Therm Eng*. 2018;130:418–28. <https://doi.org/10.1016/j.applthermaleng.2017.10.160>.
41. Yari M. Exergetic analysis of various types of geothermal power plants. *Renew Energy*. 2010;35:112–21. <https://doi.org/10.1016/j.renene.2009.07.023>.
42. Kanoglu M, Bolatturk A. Performance and parametric investigation of a binary geothermal power plant by exergy. *Renew Energy*. 2008;33:2366–74. <https://doi.org/10.1016/j.renene.2008.01.017>.
43. Zare V. A comparative exergoeconomic analysis of different ORC configurations for binary geothermal power plants. *Energy Convers Manag*. 2015;105:127–38. <https://doi.org/10.1016/j.enconman.2015.07.073>.
44. Wang S, Yuan Z, Yu N. Thermo-economic optimization of organic Rankine cycle with steam-water dual heat source. *Energy*. 2023;274:127358. <https://doi.org/10.1016/j.energy.2023.127358>.
45. Akrami E, Chitsaz A, Nami H, Mahmoudi SMS. Energetic and exergoeconomic assessment of a multi-generation energy system based on indirect use of geothermal energy. *Energy*. 2017;124:625–39. <https://doi.org/10.1016/j.energy.2017.02.006>.
46. Calise F, Capuozzo C, Carotenuto A, Vanoli L. Thermo-economic analysis and off-design performance of an organic Rankine cycle powered by medium-temperature heat sources. *Sol Energy*. 2014;103:595–609. <https://doi.org/10.1016/j.solener.2013.09.031>.
47. Gholamian E, Habibollahzade A, Zare V. Development and multi-objective optimization of geothermal-based organic Rankine cycle integrated with thermoelectric generator and proton exchange membrane electrolyzer for power and hydrogen production. *Energy Convers Manag*. 2018;174:112–25. <https://doi.org/10.1016/j.enconman.2018.08.027>.
48. Behzadi A, Gholamian E, Houshfar E, Habibollahzade A. Multi-objective optimization and exergoeconomic analysis of waste heat recovery from Tehran's waste-to-energy plant integrated with an ORC unit. *Energy*. 2018;160:1055–68. <https://doi.org/10.1016/j.energy.2018.07.074>.
49. Lan Y, Wang S, Lu J, Zhai H, Mu L. Comparative analysis of organic rankine cycle, Kalina cycle and thermoelectric generator to recover waste heat based on energy, exergy, economic and environmental analysis method. *Energy Convers Manag*. 2022;273:116401. <https://doi.org/10.1016/j.enconman.2022.116401>.
50. Ng C, Tam ICK, Wetenhall B. Waste heat source profiles for marine application of organic rankine cycle. *J Mar Sci Eng*. 2022;10:1122. <https://doi.org/10.3390/jmse10081122>.
51. Zhu S, Sun K, Bai S, Deng K. Thermodynamic and techno-economic comparisons of the steam injected turbocompounding system with conventional steam Rankine cycle systems in

- recovering waste heat from the marine two-stroke engine. *Energy*. 2022;245:123245. <https://doi.org/10.1016/j.energy.2022.123245>.
52. Scott Jenkins. 2023 CEPCI updates. *Chemical Engineering Magazine* 2023. <https://www.chemengonline.com/2023-cepci-updates-april-prelim-and-march-final/>. Accessed 5 July 2023.
  53. Elkafas AG, Rivarolo M, Massardo AF. Environmental economic analysis of speed reduction measure onboard container ships. *Environ Sci Pollut Res*. 2023. <https://doi.org/10.1007/s11356-023-26745-4>.
  54. Rutherford D, Mao X, Comer B. Potential CO<sub>2</sub> reductions under the Energy Efficiency Existing Ship Index 2020. <https://theicct.org/publication/potential-co2-reductions-under-the-energy-efficiency-existing-ship-index/>. Accessed 5 Mar 2024.
  55. IMO. Resolution MEPC.350(78): Guidelines on the method of calculation of the attained energy efficiency existing ship index (EEXI). 2022. [https://wwwcdn.imo.org/localresources/en/KnowledgeCentre/IndexofIMOResolutions/MEPCDocuments/MEPC.350\(78\).pdf](https://wwwcdn.imo.org/localresources/en/KnowledgeCentre/IndexofIMOResolutions/MEPCDocuments/MEPC.350(78).pdf). Accessed 20 Mar 2024.
  56. IMO. 2021 Guidance on Treatment of Innovative Energy Efficiency Technologies for Calculation and Verification of the Attained EEDI and EEXI. 2021. [https://wwwcdn.imo.org/localresources/en/KnowledgeCentre/IndexofIMOResolutions/MEPCDocuments/MEPC.351\(78\).pdf](https://wwwcdn.imo.org/localresources/en/KnowledgeCentre/IndexofIMOResolutions/MEPCDocuments/MEPC.351(78).pdf). Accessed 20 Mar 2024.
  57. Hung TC, Wang SK, Kuo CH, Pei BS, Tsai KF. A study of organic working fluids on system efficiency of an ORC using low-grade energy sources. *Energy*. 2010;35:1403–11. <https://doi.org/10.1016/j.energy.2009.11.025>.
  58. Chowdhury AS, Ehsan MM. A critical overview of working fluids in organic rankine, supercritical rankine, and supercritical brayton cycles under various heat grade sources. *Int J Thermofluids*. 2023;20:100426. <https://doi.org/10.1016/j.ijft.2023.100426>.
  59. Roy JP, Misra A. Parametric optimization and performance analysis of a regenerative Organic Rankine Cycle using R-123 for waste heat recovery. *Energy*. 2012;39:227–35. <https://doi.org/10.1016/j.energy.2012.01.026>.
  60. Surindra MD, Caesarendra W, Prasetyo T, Mahlia TMI, Taufik. Comparison of the utilization of 110 °C and 120 °C heat sources in a geothermal energy system using Organic Rankine Cycle (ORC) with R245fa, R123, and mixed-ratio fluids as working fluids. *Processes*. 2019;7:113. <https://doi.org/10.3390/pr7020113>.
  61. Aghahosseini S, Dincer I. Comparative performance analysis of low-temperature Organic Rankine Cycle (ORC) using pure and zeotropic working fluids. *Appl Therm Eng*. 2013;54:35–42. <https://doi.org/10.1016/j.applthermaleng.2013.01.028>.
  62. Seyedkavoosi S, Javan S, Kota K. Exergy-based optimization of an organic Rankine cycle (ORC) for waste heat recovery from an internal combustion engine (ICE). *Appl Therm Eng*. 2017;126:447–57. <https://doi.org/10.1016/j.applthermaleng.2017.07.124>.

**Publisher's Note** Springer Nature remains neutral with regard to jurisdictional claims in published maps and institutional affiliations.

Springer Nature or its licensor (e.g. a society or other partner) holds exclusive rights to this article under a publishing agreement with the author(s) or other rightsholder(s); author self-archiving of the accepted manuscript version of this article is solely governed by the terms of such publishing agreement and applicable law.